nitrogen atmosphere on the end of a glass fiber with epoxy and quickly transferred to the nitrogen stream of the cooling device. Under these conditions no crystal decay was observed during the course of the data collection. Refinement was by full-matrix least-squares techniques (241 variables) using SHELX-76. The W and O atoms were refined anisotropically, and all hydrogen atoms were placed in calculated positions (C-H = 0.95 Å) and constrained to "ride" on their respective carbon atoms. The largest peak on the final difference-Fourier map was 0.89 e/Å$^3$. An empirical absorption correction was appled on the basis of $\Psi$ scans of two reflections located near $\chi = 90°$.

**X-ray Study of W(O-2,6-$C_6H_3Me_2$)$_4$.** See Table I for details. Refinement was by full-matrix least-squares techniques (85 variables) using SHELX-76. Hydrogen atoms were ignored while all other atoms were refined anisotropically. The final difference-Fourier map contained no chemically significant electron density. A semiempirical absorption correction was applied.

**Acknowledgment.** R.R.S. thanks the National Institutes of Health for support through Grant GM-31978. We thank the Biomedical Research Support-Shared Instrumentation Grant Program, Division of Research Resources, for funds to purchase the X-ray diffraction equipment (NIH Grant S10 RR02243).

**Registry No.** *mer*-W(DMP)$_3$Cl$_3$, 102307-42-6; *trans*-W(DMP)$_4$Cl$_2$, 82972-39-2; W(DMP)$_4$, 99248-59-6; W(EtC≡CEt)(DMP)$_4$, 99248-63-2; W(O)(DMP)$_4$, 111557-27-8; W(N$_2$CHSiMe$_3$)(DMP)$_4$, 111557-26-7; W(NSiMe$_3$)(DMP)$_4$, 111557-29-0; W(S)(DMP)$_4$, 111557-28-9; W(DIPP)$_4$, 99248-58-5; WCl$_4$(Et$_2$S)$_2$, 40354-86-7; S, 7704-34-9; O$_2$, 7782-44-7; iodosylbenzene, 536-80-1; cyclohexene oxide, 286-20-4; mesitylenethiol, 1541-10-2.

**Supplementary Material Available:** Numbering scheme for carbon atoms (Figure 1) and final thermal parameters (Table S1) and final hydrogen atom positions (Table S2) for W(O-2,6-$C_6H_3$-*i*-$Pr_2$)$_4$ and final thermal parameters (Table S4) for W(O-2,6-$C_6H_3Me_2$)$_4$ (5 pages); observed and calculated structure factors for the two compounds (Tables S3 and S5) (27 pages). Ordering information is given on any current masthead page.

Contribution from the Department of Chemistry, University of Minnesota, Minneapolis, Minnesota 55455

# Reaction of $H_2S$ with $[Ir(H)_2(Me_2CO)_2(PPh_3)_2]BF_4$. Crystal and Molecular Structures of $[Ir_2(SH)_2(H)_3(PPh_3)_4]BF_4 \cdot 2(CH_3)_2CO$, $[Ir_2S(SH)(H)_3(PPh_3)_4] \cdot 1.5C_6H_6$, and $[Ir_2(SH)(SC_3H_7)(H)_3(PPh_3)_4]BF_4 \cdot (CH_3)_2CO$ and Their Reactions with Organic Reagents

Ann M. Mueting, Paul D. Boyle, Robert Wagner, and Louis H. Pignolet*

*Received July 8, 1987*

The reaction of $H_2S$ with $[Ir(H)_2(Me_2CO)_2(PPh_3)_2]BF_4$ in acetone solution led to the formation of the hydrido- and sulfhydryl-bridged dimeric complex $[Ir_2(SH)_2(H)_3(PPh_3)_4]BF_4$ (**1**) as a major product, which upon deprotonation of one bridging SH ligand produced $[Ir_2S(SH)(H)_3(PPh_3)_4]$ (**2**). A minor product isolated from the $H_2S$ reaction was the propane-2-thiolato-bridged dimeric complex $[Ir_2(SH)(SC_3H_7)(H)_3(PPh_3)_4]BF_4$ (**3**). All three complexes were characterized by single-crystal X-ray diffraction [**1**·2$(CH_3)_2CO$, triclinic $P\bar{1}$, $a = 14.919$ (8) Å, $b = 23.63$ (2) Å, $c = 18.835$ (4) Å, $\alpha = 92.09$ (5)°, $\beta = 113.95$ (4)°, $\gamma = 79.16$ (7)°, $Z = 2$, $R = 0.056$; **2**·1.5$C_6H_6$, monoclinic $P2_1/n$, $a = 17.377$ (6) Å, $b = 24.658$ (6) Å, $c = 18.220$ (5) Å, $\beta = 92.76$ (2)°, $Z = 4$, $R = 0.046$; **3**·$(CH_3)_2CO$, monoclinic $P2_1/a$, $a = 20.154$ (9) Å, $b = 18.349$ (9) Å, $c = 21.690$ (7) Å, $\beta = 108.08$ (3)°, $Z = 4$, $R = 0.046$] and $^1H$ and $^{31}P$ NMR spectroscopy. In all three complexes, the coordination geometry about each Ir atom is approximately pseudooctahedral, being bound to a terminal hydride, a bridging hydride, two cis phosphines, and two bridging sulfur atoms. The planes that contain an iridium atom and the two bound phosphines in each half of compounds **1** and **2** are approximately orthogonal, the dihedral angle equaling 82.9° in **1** and 84.0° in **2**. In **3** this angle is opened up somewhat to 108.8°. The dihedral angle between the planes containing the two iridium atoms and each sulfur atom is 73.9° in **1** and 77.0° in both **2** and **3**. Neither the iridium hydrides nor the sulfhydryl hydrogen atoms were located in the X-ray analyses of any of the complexes; however, their positions could be deduced by a combination of X-ray and NMR data. $^{31}P$ and $^1H$ NMR indicates the presence of three isomers for **1**, two isomers for **2**, and three isomers for **3** with respect to the orientation of the SR groups (R = H, $C_3H_7$) relative to the metal-metal axis. Compounds **1** and **2** reacted with various organic reagents such as $CH_2I_2$, $BrCH_2CH_2Br$, and $CH_3I$ to give high yields of products in which the sulfur ligands were alkylated.

## Introduction

Interest in the chemistry and reactivity of sulfhydryl- ($SH^-$-) containing complexes[1-12] is due in part to efforts to understand possible modes of reaction of SH groups on metal sulfide hydrodesulfurization catalysts[1,5,6] and also to their potential in serving

(1) Rakowski DuBois, M.; Casewit, C. J. *J. Am. Chem. Soc.* **1986**, *108*, 5482.
(2) Seyferth, D.; Womack, G. B.; Henderson, R. S.; Cowie, M.; Hames, B. W. *Organometallics* **1986**, *5*, 1568 and references therein.
(3) Bianchini, C.; Mealli, C.; Meli, A.; Sabat, M. *Inorg. Chem.* **1986**, *25*, 4617.
(4) Angelici, R. J.; Gingerich, R. G. W. *Organometallics* **1983**, 2, 89 and references therein.
(5) (a) Rauchfuss, T. B.; Ruffing, C. J. *Organometallics* **1982**, *1*, 400. (b) McCall, J. M.; Shaver, A. *J. Organomet. Chem.* **1980**, *193*, C37. (c) Hausmann, H.; Hofler, M.; Kruck, T.; Zimmermann, H. W. *Chem. Ber.* **1981**, *114*, 975. (d) Hofler, M.; Hausmann, H.; Heidelberg, H. A. *J. Organomet. Chem.* **1981**, *213*, C1. (e) Cooper, M. K.; Duckworth, P. A.; Henrick, K.; McPartlin, M. *J. Chem. Soc., Dalton Trans.* **1981**, 2357.
(6) (a) Schmidt, M.; Hoffmann, G. G. *Z. Anorg. Allg. Chem.* **1980**, *464*, 209. (b) Briant, C. E.; Hughes, G. R.; Minshall, P. C.; Mingos, D. M. P. *J. Organomet. Chem.* **1980**, *202*, C18. (c) Kurz, R.; Vahrenkamp, H. *J. Chem. Res., Synop.* **1982**, 30. (d) Beck, W.; Grenz, R.; Guetzfried, F.; Vilsmaier, E. *Chem. Ber.* **1981**, *114*, 3184. (e) Harris, R. O.; Yaneff, P. *J. Organomet. Chem.* **1977**, *134*, C40. (f) DiVaira, M.; Midollini, S.; Sacconi, L. *Inorg. Chem.* **1979**, *18*, 3466. (g) Gaffney, T. R.; Ibers, J. A. *Inorg. Chem.* **1982**, *21*, 2857. (h) Danzer, W.; Fehlhammer, W. P.; Liu, A. T.; Theil, G.; Beck, W. *Chem. Ber.* **1982**, *115*, 1682.
(7) (a) Vahrenkamp, H. *Angew. Chem., Int. Ed. Engl.* **1975**, *14*, 322. (b) Stiefel, E. I. *Prog. Inorg. Chem.* **1977**, *22*, 1.
(8) (a) Weberg, R. T.; Haltiwanger, R. C.; Laurie, J. C. V.; Rakowski DuBois, M. *J. Am. Chem. Soc.* **1986**, *108*, 6242. (b) Laurie, J. C. V.; Duncan, L.; Haltiwanger, R. C.; Weberg, R. T.; Rakowski DuBois, M. *J. Am. Chem. Soc.* **1986**, *108*, 6234.
(9) Seyferth, D.; Womack, G. B. *Organometallics* **1986**, *5*, 2360.

0020-1669/88/1327-0271$01.50/0 

as models for biological systems.[7] Various reports have demonstrated that sulfhydryl and disulfido ($S_2^{2-}$) ligands are highly reactive and allow the preparation of new and unusual sulfur-coordinated ligands.[4,8-10] The terminal and bridging sulfhydryl ligands have revealed a rich chemistry as a result of the ability of the coordinated SH group to add to a variety of unsaturated substrates.[1,2,4,11] This reactivity appears to depend on the metal involved,[10a] which affects the nucleophilicity of the SH ligand.[12]

Bound sulfhydryl ligands in metal complexes have been synthesized through a variety of methods that include metathetical reactions,[13] acidification[14] or hydrogenation[1,11c] of compounds containing bridging sulfur ligands, sulfur abstraction from episulfides by metal hydrides,[15] and reaction of $H_2S$ with various metal complexes.[3,16-19] Our interest has stemmed from the study of this last reaction and the conversion of $H_2S$, a product of the hydrodesulfurization reaction, to usable products such as organosulfur compounds and $H_2$.[19-21] We have therefore investigated the reaction of $[Ir(H)_2(Me_2CO)_2(PPh_3)_2]BF_4$ with $H_2S$ in acetone solution. This resulted in the formation of two sulfur- and hydrogen-bridged binuclear iridium species, $[Ir_2(SH)_2(H)_3(PPh_3)_4]BF_4$ (**1**) and $[Ir_2(SH)(SC_3H_7)(H)_3(PPh_3)_4]BF_4$ (**3**). Upon deprotonation, **1** formed the neutral analogue $[Ir_2S(SH)(H)_3(PPh_3)_4]$ (**2**), which contains one bridging sulfhydryl ligand and one bridging sulfido ligand. The reaction of $[Ir(H)_2(Me_2CO)_2(PPh_3)_2]BF_4$ with $H_2S$ was briefly reported previously[22] but was carried out in the solid state and formed the unstable complex $[Ir(H)_2(H_2S)_2(PPh_3)]BF_4$. We report here the synthesis, isolation, X-ray structural characterization, and reactions of these new and structurally similar butterfly-shaped binuclear complexes.

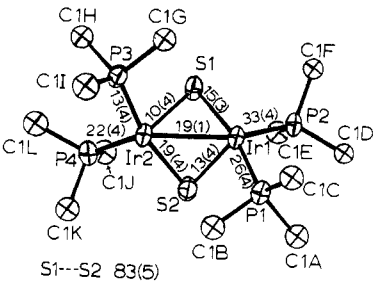


**Figure 1.** ORTEP drawing of the coordination core of $[Ir_2S(SH)(H)_3(PPh_3)_4]$ (**2**) with 50% probability ellipsoids. The labeling scheme of the protonated complex **1** is identical. The numbers are the increases in bond lengths in $10^{-3}$ Å upon protonation to give $[Ir_2(SH)_2(H)_3(PPh_3)_4]BF_4$ (**1**). The numbers in parentheses are esd's.

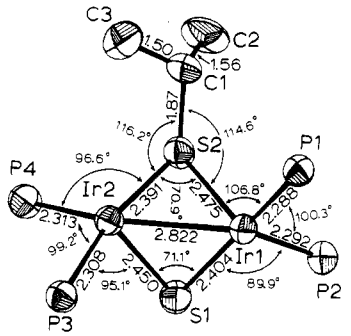


**Figure 2.** ORTEP drawing (50% ellipsoids) of the coordination core of $[Ir_2(SH)(SC_3H_7)(H)_3(PPh_3)_4]BF_4$ (**3**) with selected distances (Å) and angles (deg).

## Results and Discussion

**Syntheses and Solid-State Structures.** $[Ir_2(SH)_2(H)_3(PPh_3)_4]BF_4$ (**1**) was isolated in good yield as yellow needles from the reaction mixture of $H_2S$ and $[Ir(H)_2(Me_2CO)_2(PPh_3)_2]BF_4$ with use of acetone as solvent and was structurally characterized in the solid state by single-crystal X-ray diffraction. The structure consisted of well-separated bimetallic cations and anions with no unreasonably short intermolecular contacts. The crystal contained two acetone solvate molecules per cation, and the $BF_4^-$ anion showed the usual signs of disorder. Elemental analysis supported this formulation of **1**.

$[Ir_2S(SH)(H)_3(PPh_3)_4]$ (**2**) was formed in essentially quantitative yield from the deprotonation of **1** by NaOMe with use of benzene as solvent. Slow crystallization from benzene/hexane produced large rectangular crystals that appeared green or red, depending on the angle of observation. The crystal structure of **2** consisted of well-separated bimetallic complexes and $C_6H_6$ solvate molecules.

Also isolated (vide infra) from the reaction of $[Ir(H)_2(Me_2CO)_2(PPh_3)_2]BF_4$ with $H_2S$, and crystallized by the slow diffusion of acetone with hexane, was the yellowish orange complex $[Ir_2(SH)(SC_3H_7)(H)_3(PPh_3)_4]BF_4$ (**3**). The crystal structure of **3** consisted of well-separated cations, $BF_4^-$ anions, and acetone solvate molecules. The charge of the cation was confirmed to be 1+ by the location and refinement of one tetrafluoroborate anion per bimetallic cation and by elemental analysis. The origin of **3** will be discussed in a later section.

The molecular structures of the binuclear complexes **1** and **2** are very similar and are both represented by a perspective view of the bimetallic core of **2**, including a labeling scheme that is the same for both, in Figure 1. The structure of **3** is shown in Figure 2. Selected distances and angles for **1**–**3** are listed in Table V. The differences in bond lengths, within the coordination cores, between complexes **1** and **2** are also presented in Figure 1.

(10) (a) Angelici, R. J.; Gingerich, R. G. W. *J. Am. Chem. Soc.* **1979**, *101*, 5604. (b) Ruffing, C. J.; Rauchfuss, T. B. *Organometallics* **1985**, *4*, 524. (c) Giolando, D. M.; Rauchfuss, T. B. *J. Am. Chem. Soc.* **1984**, *106*, 6455. (d) Seyferth, D.; Womack, G. B.; Song. L.-C. *Organometallics* **1983**, *2*, 776. (e) Seyferth, D.; Womack, G. B.; Songl, L.-C.; Cowie, M.; Hames, B. W. *Organometallics* **1983**, *2*, 928. (f) Casewit, C. J.; Haltiwanger, R. C.; Noordik, J.; Rakowski DuBois, M. *Organometallics* **1985**, *4*, 119. (g) Rajan, O. A.; McKenna, M.; Noordik, J.; Haltiwanger, R. C.; Rakowski DuBois, M. *Organometallics* **1984**, *3*, 831.
(11) (a) Rauchfuss, T. B.; Ruffing, C. J. *Organometallics* **1982**, *1*, 400. (b) Rakowski Du Bois, M.; VanDerveer, M. C.; DuBois, D. L.; Haltiwanger, R. C.; Miller, W. K. *J. Am. Chem. Soc.* **1980**, *102*, 7456. (c) Seyferth, D.; Womack, G. B. *J. Am. Chem. Soc.* **1982**, *104*, 6839.
(12) Ruffing, C. J.; Rauchfuss, T. B. *Organometallics* **1985**, *4*, 524.
(13) Kopf, H.; Schmidt, M. *Angew. Chem., Int. Ed. Engl.* **1965**, *4*, 953.
(14) Noble, M. E.; Huffman, J. C.; Wentworth, R. A. D. *Inorg. Chem.* **1983**, *22*, 1756.
(15) (a) Beck, W.; Danzer, W.; Hofer, R. *Angew. Chem., Int. Ed. Engl.* **1973**, *12*, 77. (b) Beck, W.; Danzer, W.; Thiel, G. *Angew. Chem., Int. Ed. Engl.* **1973**, *12*, 582. (c) Kury, R.; Vahrenkamp, H. *J. Chem. Res., Miniprint* **1982**, 401.
(16) Mueting, A. M.; Boyle, P.; Pignolet, L. H. *Inorg. Chem.* **1984**, *23*, 44.
(17) Bottomley, F.; Drummond, D. F.; Egharevba, G. O.; White, P. S. *Organometallics* **1986**, *5*, 1620.
(18) (a) Heberhold, M.; Süss, G. *Angew. Chem., Int. Ed. Engl.* **1976**, *15*, 366. (b) Kuehn, C. G.; Taube, H. *J. Am. Chem. Soc.* **1976**, *98*, 689. (c) Behrens, H.; Lindner, E.; Lehnert, G. *J. Organomet. Chem.* **1970**, *22*, 665. (d) Ramasami, T.; Sykes, A. G. *Inorg. Chem.* **1976**, *15*, 1010. (e) Küllmer, V.; Vahrenkamp, H. *Chem. Ber.* **1977**, *110*, 3799, 3810. (f) Schmidt, M.; Hoffman, G. G. *Z. Anorg. Allg. Chem.* **1980**, *464*, 209. (g) Briant, C. E.; Hughes, G. R.; Minshall, P. C.; Mingos, D. M. P. *J. Organomet. Chem.* **1980**, *202*, C18. (h) Singer, H.; Wilkinson, G. *J. Chem. Soc. A* **1968**, 2516. (i) Vaska, L. *J. Am. Chem. Soc.* **1966**, *88*, 5325. (j) Dirand, J.; Ricard, L.; Weiss, R. *Inorg. Nucl. Chem. Lett.* **1975**, *11*, 661. (k) Roper, W. R. *J. Chem. Soc., Dalton Trans.* **1973**, 1014. (l) Ugo, R. *J. Chem. Soc., Chem. Commun.* **1967**, 524. (m) Robertson, H. *J. Chem. Soc., Dalton Trans.* **1978**, 753. (n) Vidal, J. L. *Inorg. Chem.* **1978**, *17*, 2574. (o) Adams, R. D.; Horvath, I. T.; Yang, L.-W. *Organometallics* **1983**, *2*, 1257. (p) Midollini, S.; et al. *Transition Met. Chem. (Weinhein, Ger.)* **1983**, *8*, 73. (q) Midollini, S.; et al. *Inorg. Chem.* **1983**, *22*, 3802. (r) Werner, H.; Bertleff, W.; Schubert, U. *Inorg. Chim. Acta* **1980**, *43*, 199. (s) Osakada, K.; Yamamoto, T.; Yamamoto, A. *Inorg. Chim. Acta* **1984**, *90*, L5. (t) Osakada, K.; Yamamoto, T.; Yamamoto, A.; Takenaka, A.; Sasada, Y. *Inorg. Chim. Acta* **1985**, *105*, L9.
(19) (a) Lee, C.-L.; Besenyei, G.; James, B. R.; Nelson, D. A.; Lilga, M. A. *J. Chem. Soc., Chem. Commun.* **1985**, 1175. (b) Lee, C.-L.; Chisholm, J.; James, B. R.; Nelson, D. A.; Lilga, M. A. *Inorg. Chim. Acta* **1986**, *121*, L7.
(20) Bianchini, C.; Mealli, C.; Meli, A.; Sabat, M. *Inorg. Chem.* **1986**, *25*, 4617.
(21) Bottomley, F.; Drummond, D. F.; Egharevba, G. O.; White, P. S. *Organometallics* **1986**, *5*, 1620.
(22) Crabtree, R. H.; Davis, M. W.; Mellea, M. F.; Mihelcic, J. M. *Inorg. Chim. Acta* **1983**, *72*, 223.

$^1H$ NMR established the presence of one bridging hydride $H_b$, two terminal hydrides $H_t$, and two bridging SH hydrogens in **1** (only one bridging SH group in **2** and **3**). No hydrogens were

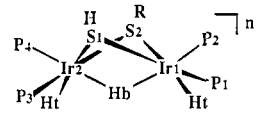


**1** (R = H, $n$ = +1), **2** (R = vacant, $n$ = 0), **3** (R = $HC(CH_3)_2$, $n$ = +1)

located in the final difference Fourier maps, but their positions were inferred from the structural and NMR data (vide infra). The overall stereochemistry of these complexes is quite similar to that of $[Ir_2(\mu\text{-}H)_3(H)_2(PPh_3)_4]PF_6$[23] and $\{[Ir(H)(\mu\text{-S-}t\text{-Bu})(CO)(PR_3)]_2(\mu\text{-}H)\}ClO_4$,[24,25] for which the hydride positions have also been inferred. The proposed hydrogen placements are shown above, and details of the NMR evidence will be presented in a later section. Each terminal hydride, one per iridium, occupies the vacant position approximately trans to one of the bridging sulfur ligands and cis to the $PPh_3$ ligands. The stereochemistry about each iridium atom is therefore approximately octahedral, as expected for Ir(III). The sulfur groups symmetrically bridge the two iridium atoms. Hydrogens are bonded to both sulfur bridges in **1** and to only one in **2**. In **3** an isopropyl group is attached to one sulfur bridge and a hydrogen atom to the other.

Each iridium atom lies in a distorted pseudooctahedral environment, both octahedra sharing the face [S1, S2, $H_b$]. The most significant distortion from pseudooctahedral geometry in **1** and **2** is a result of steric repulsion between the bulky cis $PPh_3$ groups and the close proximity of the iridium atoms as required by the bridging groups. Thus, the S2–Ir1–P2 and S1–Ir2–P4 angles are 108.6 (1) and 110.0 (1)° in **1** and 108.2 (1) and 108.0 (1)° in **2**, respectively. The P1–Ir1–P2 and P3–Ir2–P4 angles are 104.1 (1) and 104.2 (2)° in **1** and 104.3 (1) and 105.7 (1)° in **2**, respectively. Similarly, the most significant distortion in **3** is a result of the steric repulsion between the bulky cis $PPh_3$ groups, the isopropyl group on the sulfur, and the close proximity of the iridium atoms. Thus, the S2–Ir1–P1, S2–Ir1–P2, and S2–Ir2–P4 angles are 106.8 (1), 108.2 (1), and 96.6 (1)°, respectively. The P1–Ir1–P2 and P3–Ir2–P4 angles in **3** are 100.3 (1) and 99.2 (1)°. The large isopropyl group, therefore, plays a significant role in decreasing the angle between the $PPh_3$ groups.

The dihedral angle between the two planes containing [Ir1–P1–P2] and [Ir2–P3–P4] is 82.9° in **1** and 84.0° in **2** and is opened up to 108.8° in **3**, again due to the steric repulsion between the isopropyl group and the $PPh_3$ groups. The dihedral angle between the two planes containing [Ir1–S1–Ir2] and [Ir1–S2–Ir2] is 73.9° in **1** and 77.0° in both **2** and **3**. The intramolecular S1···S2 separation is 3.193 (5) Å in **1**, 3.110 (5) Å in **2**, and 3.098 (4) Å in **3**, consistent with nonbonding interactions.[16,26] The Ir1···Ir2 separation (2.796 (1) Å in **1**, 2.777 (1) Å in **2**, and 2.822 (1) Å in **3**) suggests a bonding interaction; however, the short distance is more likely to be a result of the geometrical requirements of the bridging hydride, as in $[Ir_2(H)_5(PPh_3)_4]PF_6$ (2.52 Å).[23] Complexes with only bridging SR groups exist either with a normal 2e Ir–Ir bond as in $[Ir^{II}(H)(\mu\text{-S-}t\text{-Bu})(CO)(P(OMe)_3)]_2$ (2.673 (1) Å) or with no Ir–Ir interaction as in $[Ir^{I}(\mu\text{-S-}t\text{-Bu})(CO)(P(OMe)_3)]_2$ (3.216 (2) Å), depending upon the electronic requirements of the metals.[24] Therefore, it is apparent that the bridging hydride requires the Ir atoms to be close, and it is probably best to describe the bonding as a M–H–M two-electron, three-center bridge bond.

The average Ir–S distance (2.431 Å) in all three complexes compares well with the average Ir–S distance (2.436 (2) Å) in the SR-bridged complex $[IrI(\mu\text{-S-}t\text{-Bu})(CO)P(OMe)_3]_2[\mu\text{-}CH_2]$.[25] The Ir–S bond distances do not seem to be governed by the nature of the attached group as much as they are affected by the ligand in the trans position. For example, the Ir–S bonds in **3** that are attached to the isopropyl group (average 2.433 (3) Å) show no significant differences from the Ir–S bonds attached to hydrogen (average 2.427 (3) Å). However, the Ir–S bonds trans to the hydride ligands are significantly longer than the Ir–S bonds trans to the $PPh_3$ ligands due to the stronger structural trans influence of the terminal hydride ligands.[27] For example, the Ir2–S1 bond distance of 2.459 (4) Å trans to the hydrido ligand in complex **1** is significantly longer than the Ir2–S2 distance of 2.415 (4) Å trans to $PPh_3$. Respective distances in **2** are 2.449 (4) and 2.396 (4) Å and in **3** are 2.450 (3) and 2.391 (3) Å. The Ir–P distances (average 2.289 Å in **1**, 2.267 Å in **2**, and 2.300 Å in **3**) compare well with values observed in other Ir(III) phosphine complexes (range 2.25–2.42 Å).[28] There are no significant differences seen between the Ir–P bonds trans to the bridging hydride and those trans to the bridging sulfur ligands. This is not unusual since bridging hydrides, in contrast to the case for terminal hydrides, do not exhibit a large trans influence.[29]

In **3** the S2–C1 bond distance (1.87 (1) Å) compares well with the S–C bond distance (1.85 (2) Å) in the S-*t*-Bu-bridged complex $[Ir(H)(\mu\text{-S-}t\text{-Bu})(CO)(P(OMe)_3]_2$.[24] The angles around the bridging S atom bonded to the isopropyl group are in agreement with approximately $sp^3$ hybridization but are distorted because of the shortness of the Ir···Ir separation (Ir1–S2–C1 = 114.6 (4)°, Ir2–S2–C1 = 116.2 (4)°, and Ir2–S2–Ir1 = 70.88 (7)°).

The conversion of the monocation **1** to the neutral species **2** involves the loss of one SH proton and is reversible upon the addition of $HBF_4$. With the protonation of the bridging sulfide in **2**, the bonds, as well as the nonbonding distances, in the main coordination sphere increase in length to a significant extent. These changes in distances are all positive upon protonation (i.e., in going from **2** to **1**) and are shown in Figure 1. The Ir···Ir distance increased by 0.019 (1) Å and the S···S distance by 0.083 (5) Å. The four Ir–S bonds increased to a similar extent with an average increase of 0.014 (4) Å and provide no clear indication as to which sulfur atom in **2** is unprotonated. The sulfur atoms were refined without signs of disorder, but the fact that there was no difference seen in the change in the lengths of the bonds to one bridging sulfur ligand vs the other suggests the possibility of disorder between S and SH in **2**. The increase in the Ir–P distances ranged from 0.013 (4) to 0.033 (4) Å, the greater changes occurring in the ligands trans to the bridging hydride. The P–C bond lengths in the $PPh_3$ ligands in both complexes are not significantly affected by the protonation and average 1.84 and 1.84 Å in **1** and **2**, respectively.

The conversion of **2** to **1** involves no change in the number of electrons, only in the number of SH protons and therefore charge. This increase in the overall charge on the molecule appears to be delocalized from the sulfur ligand to the more electropositive iridium atoms, resulting in a slight decrease in the bonding interactions. The difference in color of the two complexes, green in **2** ($\lambda_{max}$ = 317 nm, $\epsilon$ = 9300 $M^{-1}$ $cm^{-1}$) and yellow in **1** ($\lambda_{max}$ = 322 nm, $\epsilon$ = 13 100 $M^{-1}$ $cm^{-1}$, and $\lambda_{max}$ = 360 nm, $\epsilon$ = 5900 $M^{-1}$ $cm^{-1}$) supports this since a ligand to metal charge-transfer transition is expected to decrease in energy upon going from a neutral to a positively charged species.

The conversion of the monocation **1** to the neutral species **2** occurred not only upon deprotonation with base but also by chemical reduction with sodium naphthalenide or Na/Hg. Similarly, the yellow complex **1** could be electrochemically reduced. The cyclic voltammogram (range −1.8 to +0.5 V, scan rate 500

(23) Crabtree, R. H.; Felkin, H.; Morris, G. E. *J. Organomet. Chem.* **1977**, *141*, 205.
(24) Bonnet, J. J.; Thorez, A.; Maisonnat, A.; Galy, J.; Poilblanc, R. *J. Am. Chem. Soc.* **1979**, *101*, 5940.
(25) El Amane, M.; Maisonnat, A.; Dahan, F.; Pince, R.; Poilblanc, R. *Organometallics* **1985**, *4*, 773.
(26) Bonnet, J. J.; Kalck, P.; Poilblanc, R. *Inorg. Chem.* **1977**, *16*, 1514.
(27) Frenz, B. A.; Ibers, J. A. *Transition Metal Hydrides*; Muetterties, E. L., Ed.; Marcel Dekker: New York, 1971; pp 41–44.
(28) (a) Bau, R.; Teller, R. G.; Kirtley, S. W.; Koetzle, T. F. *Acc. Chem. Res.* **1979**, *12*, 176. (b) Debaerdemaeker, T. *Cryst. Struct. Commun.* **1977**, *6*, 11. (c) Roberts, P. J.; Ferguson, G. *Acta Crystallogr., Sect. B: Struct. Crystallogr. Cryst. Chem.* **1976**, *B32*, 1513.
(29) Immirzi, A.; Porzio, W.; Bachechi, F.; Zambonelli, L.; Venanzi, L. M. *Gazz. Chim. Ital.* **1983**, *113*, 537.

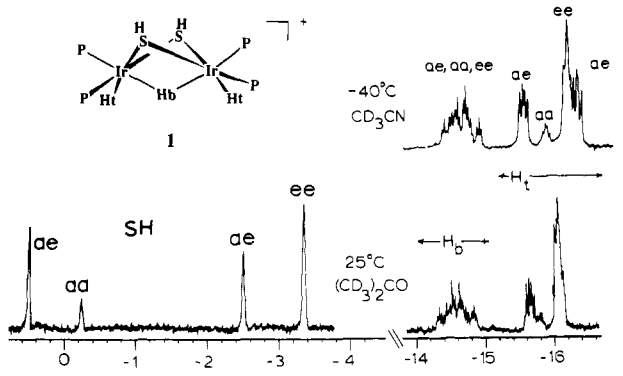


**Figure 3.** $^1H$ NMR spectra of $[Ir_2(SH)_2(H)_3(PPh_3)_4]BF_4$ (**1**) with use of acetone-$d_6$ at room temperature in the sulfhydryl and hydride regions and $CD_3CN$ at −40 °C in the hydride region. Isomer designations refer to drawings in the text.

mV/s) of a 0.6 mM solution of **1** with use of an acetone solution 0.1 M in TBAH exhibited irreversible behavior with a reduction wave at −1.63 V followed by a small oxidation return wave at about 0 V. Controlled-potential reduction of **1** at −1.7 V resulted in formation of compound **2**. Cyclic voltammetry of the resulting green solution showed an irreversible oxidation wave at −0.08 V. An authentic sample of **2** gave an identical result. The determination of $n$ by a potential-step experiment ($E_i$ = −1.70 V to $E_f$ = −1.80 V, $[[Ir_2(SH)_2(H)_3(PPh_3)_4]^+]$ = 0.6 mM) resulted in an effective $n$ value of 1.

**NMR Spectra. $[Ir_2(SH)_2(H)_3(PPh_3)_4]BF_4$ (1)** was examined by $^1H$ NMR spectroscopy with the use of acetone-$d_6$, $CD_3CN$, and DMSO-$d_6$ solvents at several temperatures. The spectra were complex due to the presence of stereoisomers but are consistent with the basic solid-state structure. Three isomeric possibilities exist that result from the stereochemistry about the SH bridging groups as shown in drawings ae, ee, and aa. These isomers have been observed before in SR-bridged compounds.[2,30]

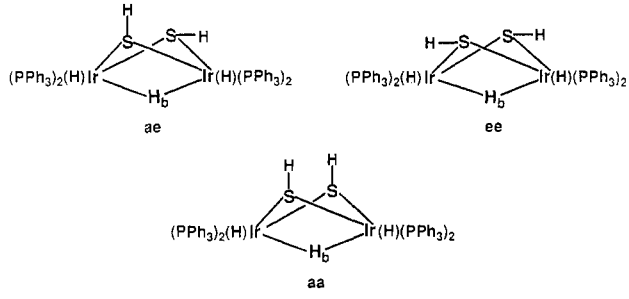


The room-temperature spectrum of the SH and the hydride region and the −40 °C spectrum of the hydride regions are reproduced in Figure 3. At −40 °C in $CD_3CN$ all of the resonances of the terminal hydrides, $H_t$, of the three possible isomers were resolved, while the resonances of the bridging hydrides, $H_b$, were partially overlapping. The SH region of the $^1H$ NMR spectrum, +2 to −4 ppm, showed well-resolved resonances of the three isomers.

In the room-temperature $^1H$ NMR spectrum of **1** (see Figure 3) the peaks at $\delta$ 0.50 and −2.51 represent SH protons of the ae isomer, the peak at $\delta$ −3.36 is due to the ee isomer, and that at −0.24 represents the aa isomer, which are present in a ratio of 9:7:1. This assignment is reasonable and was based on the relative intensities of the SH signals and comparison with the intensities and coupling patterns of the hydride signals. Generally, for analogous complexes with SR ligands only two of the isomers have been detection in solution.[31] Unfavorable van der Waals contacts have been calculated[32] for the axial–axial (aa) isomer of $[Fe(SC_2H_5)(CO)_3]_2$,[33] precluding its existence in solution, unless there exist more highly unfavorable steric interactions between the SR group and other bulky ligands.[34] Therefore, the SH resonance with the smallest relative intensity has been assigned to the aa isomer. In the ae isomer the two SH groups are nonequivalent. The hydride signal at $\delta$ −14.56 results from the overlap of the resonances of the bridging hydride $H_b$ of all three isomers. Each individual isomer gives a triplet of triplets resulting from the coupling to two equivalent trans $PPh_3$ groups ($J_{trans\text{-}P\text{-}H} \approx 59$ Hz) and two cis $PPh_3$ ligands ($J_{cis\text{-}P\text{-}H} \approx 10$ Hz). No H–H coupling was resolved since it is normally very small ($J_{H\text{-}H} < 10$ Hz) in metal hydrides and is rarely observed.[35] The remaining hydride resonances represent the terminal hydrides of the three isomers. The terminal hydrides of the aa isomer are equivalent and appear as a doublet of doublets at $\delta$ −15.86. The major peak at $\delta$ −16.13 is actually two overlapping resonances and is better resolved in the −40 °C $CD_3CN$ spectrum. Both appear as a doublet of doublets or pseudotriplet, with the larger peak being assigned to the equivalent terminal hydrides of the equatorial–equatorial (ee) isomer. The smaller underlying resonance can be assigned along with the peak at $\delta$ −15.65 to the inequivalent hydrides of the axial–equatorial (ae) isomer. All of the observed spin–spin coupling in these terminal hydride resonances results from P–H interaction. Each terminal hydride is cis to two $PPh_3$ ligands and is coupled to each to a slightly different degree, resulting in the coupling patterns observed. All of the $J_{cis\text{-}P\text{-}H}$ coupling constants range from 10 to 20 Hz and fall within the normal range of 10–30 Hz as expected for the proposed bonding modes. The $J_{trans\text{-}P\text{-}H}$ coupling constants of approximately 60 Hz observed in these isomers are in the range expected for bridging hydrides where reduced bond orders are present.[36] Note that the bridging hydrides resonate at lower field (−14 to −15 ppm) than the terminal hydrides (−15 to −16 ppm), which is consistent with the case for known polyhydrido clusters that contain only phosphine or phosphite ligands but contrary to the case for numerous other polyhydrido carbonyl cluster compounds.[36]

The $^{31}P$ NMR spectrum of **1** was complex due to the presence of the three isomers but is consistent with the formulation of **1**, and together with the $^1H$ NMR, elemental analysis, and infrared data it supports the molecular structure of **1** as shown.

**$[Ir_2(S)(SH)(H)_3(PPh_3)_4]$ (2)** was examined by $^1H$ NMR spectroscopy with use of benzene-$d_6$ or toluene-$d_8$ as solvent at several temperatures (see Figure S3 in the supplementary material). The 25 °C spectrum showed two peaks of approximately equal intensity in the SH region at $\delta$ 0.39 and −0.91 that indicates the presence of two different isomeric forms of approximately equal concentration resulting from the stereochemistry about the bridging SH group, in which the proton can be axial or equatorial. The bridging and terminal hydrides can be assigned as with **1**, but the spectrum was complicated. (See the supplementary material for a detailed analysis of the spectra and the assignments.) When **2** was warmed to 120 °C, the two SH signals broadened and coalesced to a broad average resonance at $\delta$ −0.26. The terminal hydride signals coalesced to a broad resonance centered at $\delta$ −15.2. The bridging hydride resonances of the two isomers similarly coalesced to one triplet of triplets at $\delta$ −13.05. This indicates that the isomers are interconverting and averaging the SH protons. Also, since the terminal hydrides in both isomers are averaging, it indicates that the SH proton is exchanging between the two sulfur ligands. The exact mechanism by which this is occurring is unclear, however.

As in **1**, the $^{31}P$ NMR assignment of complex **2** is not inconsistent with the proposed structure but is complicated by the presence of the two isomers. These $^{31}P$ and $^1H$ NMR data together with the elemental analysis and infrared data are consistent

(30) Seyferth, D.; Henderson, R. S. *J. Organomet. Chem.* **1981**, *218*, C34.
(31) King, R. B. *J. Am. Chem. Soc.* **1962**, *84*, 2460.
(32) Dahl, L. F.; Wei, C. H. *Inorg. Chem.* **1963**, *2*, 328.
(33) Connelly, N. G.; Johnson, G. A.; Kelley, B. A.; Woodward, P. *J. Chem. Soc., Chem. Commun.* **1977**, 436.
(34) Broadhurst, P. V.; Johnson, B. F. G.; Lewis, J. *J. Chem. Soc., Dalton Trans.* **1982**, 1881.
(35) Kaesz, H. D.; Saillant, R. B. *Chem. Rev.* **1972**, *72*, 231.
(36) Wang, H. H.; Pignolet, L. H. *Inorg. Chem.* **1980**, *19*, 1470 and references therein.

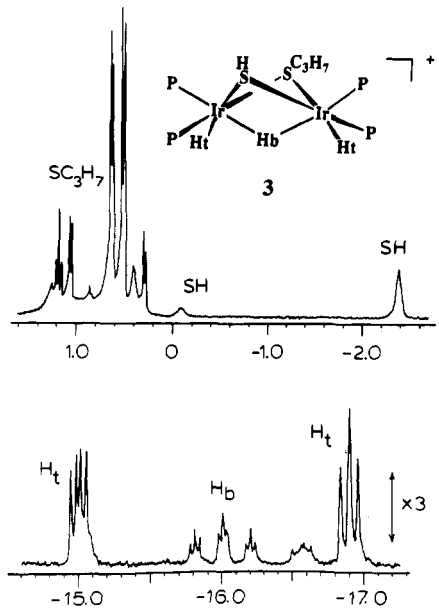


3

**Figure 4.** $^1H$ NMR spectrum of $[Ir_2(SH)(SC_3H_7)(H)_3(PPh_3)_4]BF_4$ (**3**) with use of $CD_3CN$ as solvent as room temperature showing only the hydride, SH, and isopropyl $CH_3$ regions. See text for assignments.

with the formulation and molecular structure of **2** as shown, with one SH and one S as bridging ligands.

**$[Ir_2(SH)(SC_3H_7)(H)_3(PPh_3)_4]BF_4$ (3)** was examined by $^1H$ NMR spectroscopy with use of acetone-$d_6$ or $CD_3CN$ as solvent at several temperatures. The spectrum taken at room temperature with use of $CD_3CN$ is reproduced in Figure 4. The SH and SR region of the $^1H$ NMR spectrum, +3 to −4 ppm, showed the presence of three different isomeric forms resulting from the stereochemistry about the SH and SR bridging groups. The SH protons of two of the isomers are assigned to the peaks at $\delta$ −2.4 and −0.1. The signal at $\delta$ 0.4 is due to the SH proton of the third isomer overlapped with one of the isopropyl $CH_3$ doublets. The variable-temperature spectra of this region showed a shift of the SH protons upon warming, confirming this assignment, since the peak at $\delta$ 0.4 became a sharp doublet with no other changes seen in that region. The six doublets in this region are due to isopropyl $CH_3$ resonances of the three isomers. Note that in addition to the broadened signal at $\delta$ 0.4 due to an overlapping SH resonance, the signal at $\delta$ 1.2 is complicated by an overlapping resonance due to a minor impurity in the compound. The splitting ($J$ = 6–7 Hz) is presumably a result of coupling to the isopropyl proton on the tertiary carbon since long-range coupling to the trans $PPh_3$ ligand was ruled out by a selective phosphorus-decoupling experiment. On the basis of steric arguments the major isomer is considered to be ae, in which the isopropyl group is in the axial position, thus diminishing unfavorable interactions with the $PPh_3$ ligands. The two doublets at $\delta$ 0.7 and 0.5 ($J \approx 6$ Hz) and the SH resonance at $\delta$ −2.4 are assigned to this isomer, based on integration values. The resonances attributed to the minor isomers are at $\delta$ 1.2 and 1.1 (d, $J \approx 6$ Hz) and at $\delta$ 0.4 (broad) and 0.3 (d, $J \approx 6$ Hz). The isopropyl proton attached to the tertiary carbon should appear as a multiplet for each isomer due to coupling to the methyl groups but was difficult to assign because of signals due to solvent impurities. A tentative assignment could be made, however, if the resonances due to the three isomers overlapped, as there was a multiple resonance seen at $\delta$ 1.8 (not shown in Figure 4) of approximately the appropriate intensity. The triplet of triplets at $\delta$ −16.0 results from the bridging hydride $H_b$ coupled to two trans $PPh_3$ groups ($J_{trans\text{-}P\text{-}H}$ = 59 Hz) and two cis $PPh_3$ ligands ($J_{cis\text{-}P\text{-}H}$ = 9 Hz). As in the $^1H$ NMR spectra of complexes **1** and **2**, no H–H coupling was seen. The remaining hydride resonances represent the terminal hydrides of the three possible isomers. The terminal hydrides of the major isomer appear as a doublet of doublets at $\delta$ −15.1 ($J_{cis\text{-}P\text{-}H}$ = 19 and 12 Hz) and as a pseudotriplet at $\delta$ −16.9 ($J_{cis\text{-}P\text{-}H}$ = 18 Hz). The remaining resonances due to the terminal hydrides of the other isomers were weak, underlying the major peaks. These signals shifted and could be seen in the variable-temperature spectra. Each terminal hydride is cis to two $PPh_3$ ligands and is coupled to each to a slightly different degree, resulting in the coupling patterns observed. As in **1** and **2**, all of the coupling constants fall within the normal ranges.

The $^{31}P$ NMR spectrum of **3** with use of $CD_3CN$ as solvent was complex due to the presence of isomers, but on the basis of analysis of the $^1H$ spectra with selective $^{31}P$ decoupling, assignments could be made. (See the supplementary material for traces of the spectra and the details of the analysis.) The elemental analysis, infrared spectra, and reactivity provided additional support for the formulation and molecular structure of this complex. For example, NaOMe reacted with **3** to produce a green complex. The proposed formulation of this product is $[Ir_2(S)(SC_3H_7)(H)_3(PPh_3)_4]$ (**4**), analogous to complex **2**. $^{31}P$ and $^1H$ NMR indicated the presence of one major isomer, possibly the axial isomer, and a small concentration of another (see Experimental Section). Further studies with **4** have not been carried out.

**Mechanistic Aspects of the $H_2S$ Reaction.** Compounds **1** and **3** were formed by the reaction of $H_2S$ with $[Ir(H)_2(Me_2CO)_2(PPh_3)_2]BF_4$ with use of acetone as the solvent. In an effort to understand the reactions that lead to the formation of **1** and **3**, the reaction was also carried out with use of $CD_2Cl_2$ as solvent and monitored immediately by $^1H$ NMR. In this case several intermediates were observed and one was isolated, and **3** was not formed. The initial product observed displayed a triplet resonance at $\delta$ −17.13 ($J$ = 15 Hz) and was isolated in a subsequent experiment as a pale yellow unstable powder. The IR spectrum in the solid state indicated the presence of SH or $H_2S$ ligands [$\nu$(SH) = 2520 $cm^{-1}$], hydrides [$\nu$(IrH) = 2170 $cm^{-1}$], and the $BF_4^-$ counterion [$\nu$(BF) = 1050 $cm^{-1}$]. These data compare well with those of the previously reported product of the same reaction that was carried out in the solid state.[22] The proposed product was the monomer $[Ir(H)_2(H_2S)_2(PPh_3)_2]BF_4$. When the in situ reaction in $CD_2Cl_2$ was followed with $^1H$ NMR, other products were seen to grow in with time, all of which appeared as either triplets or triplets of doublets. After several days the peak at $\delta$ −17.13 had been replaced, as the major resonance, by a triplet at $\delta$ −15.30 ($J$ = 15 Hz). This same resonance was seen as the initial reaction product of $[Ir(H)_2((CD_3)_2CO)_2(PPh_3)_2]BF_4$ with $H_2S$ in acetone-$d_6$. This triplet signal at $\delta$ −15.30 is most likely due to the oxidative-addition adduct $[Ir(SH)(H)_3(PPh_3)_2]BF_4$. This compound could dimerize to produce the yellow sulfhydryl-bridged dimer $[Ir_2(SH)_2(H)_3(PPh_3)_4]BF_4$, after the loss of $H_2$ (the evolution of gas bubbles from the reaction mixture was observed) and $H^+$. The reaction in $CD_2Cl_2$ was very slow and eventually did form complex **1** when exposed to air.

It is known that thiols react with aldehydes and ketones to form thioacetals and thioketals in acidic media. Similarly, the mononuclear complex $W(CO)_5(SH)^-$ reacts rapidly with ketones upon the addition of acid to give the thioketone complex $W(CO)_5(S{=}CR_2)$.[10a] On this basis, it is possible that the "Ir–thiol" intermediate $[Ir(SH)(H)_3(PPh_3)_2]^+$ in the slightly acidic solution reacted with the solvent acetone to form an analogous complex, which could then react with another molecule of $[Ir(SH)(H)_3(PPh_3)_2]^+$, lose a molecule of $H_2$ and $H^+$, and form the isopropyl-bridged Ir dimer $[Ir_2(SH)(SC_3H_7)(H)_3(PPh_3)_4]^+$ (**3**). An alternate mechanism in which $H_2S$ attacks the coordinated acetone, resulting in the formation of **3**, can also not be ruled out.

**Reactivity.** The complex $[Fe_2(\mu\text{-}SH)_2(CO)_6]$ undergoes a variety of reactions that mimic the reactivity of organic thiols,[2,11c,30] as for example the base-induced addition of $CH_2I_2$ and the addition to $\alpha,\beta$-unsaturated organic systems such as methyl vinyl ketone to produce alkylthio ligands. Similarly, the disulfide analogue $[Fe_2(\mu\text{-}S_2)(CO)_6]$ displays reactivity patterns that mimic those of organic disulfides.[2,10d] The complexes $[Ir_2(SH)_2(H)_3(PPh_3)_4]BF_4$ (**1**) and $[Ir_2(S)(SH)(H)_3(PPh_3)_4]$ (**2**) also mimic the reactivity of organic thiols but are not as reactive as the analogous Fe complexes. Several examples of this are presented below. Details of the reactions and spectral analysis are given in the

**Scheme I**

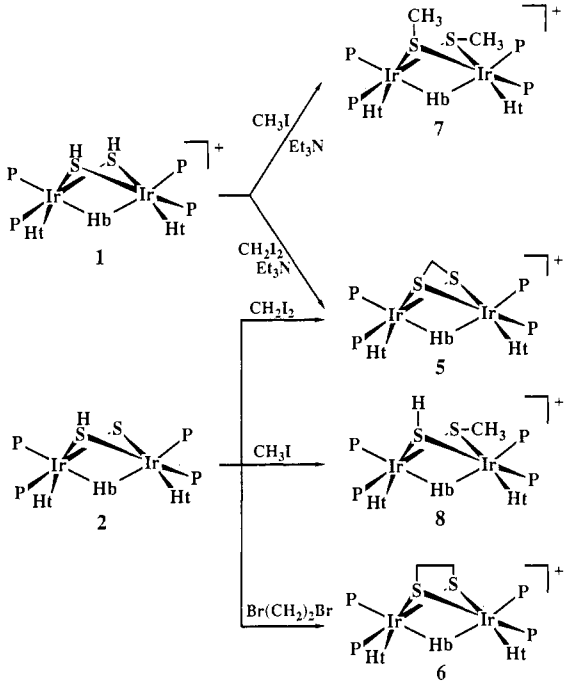


Experimental Section. A summary of the reactions is given in Scheme I.

The cationic complex **1** reacted with $CH_2I_2$ in the presence of base and the neutral dimer **2** reacted with $CH_2I_2$ unassisted by base to give the acetone-soluble product $[(\mu\text{-}SCH_2S)Ir_2(H)_3(PPh_3)_4]^+$ (**5**). NMR spectra of **5** were much simpler than for **1** or **2** since **5** cannot have isomeric forms. The $^{31}P$ NMR spectrum showed two signals of equal intensity at $\delta$ 6.43 and 5.04 corresponding to the two phosphorus environments. The $^1H$ NMR spectrum displayed a resonance at $\delta$ −11.60 that can be assigned to the bridging hydride $H_b$, split into a triplet by the two trans $PPh_3$ groups ($J_{trans\text{-}P\text{-}H}$ = 59 Hz) and further split into a triplet by the two cis $PPh_3$ ligands ($J_{cis\text{-}P\text{-}H}$ = 10 Hz). A doublet of doublets appeared at $\delta$ −17.79 due to the two terminal hydrides, each of which couple to two inequivalent cis $PPh_3$ ligands ($J_{cis\text{-}P\text{-}H}$ = 23 and 14 Hz). The resonance attributed to the $S_2CH_2$ group was at $\delta$ 6.09. This assignment was based on integration values (1.8:1:2 $SCH_2S$:$H_b$:$H_t$) and analogy to $[Fe_2(SCH_2S)(CO)_6]$ ($\delta_{SCH_2S}$ = 4.9).[37] These data are entirely consistent with the formulation of **5**.

The reaction between **2** and $Br(CH_2)_2Br$ in either toluene or benzene solution produced a pale yellow precipitate of the cationic complex $[Ir_2(SCH_2CH_2S)(H)_3(PPh_3)_4]^+$ (**6**) in high yield. The $^{31}P$ NMR spectrum with use of acetone as solvent showed two peaks of equal intensity at $\delta$ 7.43 and 7.31. The hydride region of the $^1H$ NMR spectrum with use of acetone-$d_6$ as solvent displayed two overlapping resonances, a triplet of triplets at $\delta$ −14.74, which can be attributed to the bridging hydride Ir−$H_b$ ($J_{trans\text{-}P\text{-}H}$ = 47 Hz, $J_{cis\text{-}P\text{-}H}$ = 10 Hz), and a doublet of doublets at $\delta$ −15.01, which can be assigned to the two terminal hydrides coupled to two inequivalent cis $PPh_3$ ligands ($J_{cis\text{-}P\text{-}H}$ = 25 and 13 Hz). The integration was calculated to be 1:1.7 Ir−$H_b$:Ir−$H_t$, when overlap was accounted for. There was a broad singlet at $\delta$ 6.90, which was integrated to 6 but was overlapping with the phenyl region, and by analogy to the position of the $S_2CH_2$ group in **5** this signal can be assigned to the bridging $SCH_2CH_2S$ group. These data fit well with the formulation of **6**. The reaction of $Br(CH_2)_2Br$ with **1** in acetone solution was more complicated, as indicated by $^{31}P$ and $^1H$ NMR spectroscopy. In addition to **6**, a secondary product was observed that could not be isolated or definitively characterized.

Complex **1** reacted with $CH_3I$ in the presence of $Et_3N$ in acetone solution to form the axial–equatorial isomer of $[Ir_2(SCH_3)_2(H)_3(PPh_3)_4]^+$ (**7**). Similarly, **2** reacted with *n*-BuLi in THF solution at −78 °C to presumably form the monoanion $[Ir_2(S)_2(H)_3(PPh_3)_4]^-$, which then reacted with $CH_3I$ upon warming to 25 °C to form the same ae isomer, **7**. The $^{31}P$ NMR spectrum of the isolated yellow precipitate of **7** with use of acetone as solvent showed four signals of equal intensity at $\delta$ 11.23, 5.98, 1.11, and −3.53. The $^1H$ NMR spectrum of **7** with use of acetone-$d_6$ as solvent showed two doublets of equal intensity at $\delta$ 1.09 ($J$ = 5 Hz) and 0.74 ($J$ = 5 Hz) and are assigned to the $SCH_3$ groups. The splitting presumably resulted from long-range coupling to a trans $PPh_3$ ligand for each $SCH_3$ group. The hydride region displayed a triplet of triplets at $\delta$ −14.43 ($J_{trans\text{-}P\text{-}H}$ = 60 Hz, $J_{cis\text{-}P\text{-}H}$ = 10 Hz) that can be assigned to the bridging hydride and two doublets of doublets at $\delta$ −15.57 ($J_{cis\text{-}P\text{-}H}$ = 22 and 13 Hz) and −16.08 ($J_{cis\text{-}P\text{-}H}$ = 23 and 15 Hz) that can be assigned to the inequivalent terminal hydrides. The presence of two terminal hydride resonances and two $SCH_3$ signals supports the formulation as the ae isomer, which would be the most sterically favored. Integration of the $^1H$ NMR spectrum was 1:2.4:6.5 $H_b$:$H_t$:$SCH_3$.

In contrast, the reaction of the neutral dimer **2** with either $CH_3I$ or methyl triflate in benzene solution yielded, as the major product, the axial–equatorial isomer of $[Ir_2(SH)(SCH_3)(H)_3(PPh_3)_4]^+$ (**8**). The $^{31}P$ NMR spectrum of **8** showed four major signals of equal intensity at $\delta$ 13.5, 12.2, 4.8, and 4.5. The $^1H$ NMR spectrum with use of acetone-$d_6$ as solvent showed the presence of several products. The major signals at $\delta$ 0.58 ($SCH_3$, d, $J$ = 6 Hz, int = 2.7), −0.07 (SH, br s, int = 0.8), −14.37 (Ir−$H_b$, t of t, $J_{trans\text{-}P\text{-}H}$ = 59 Hz, $J_{cis\text{-}P\text{-}H}$ = 9 Hz, int = 1.0), −15.22 (Ir−$H_t$, d of d, $J_{cis\text{-}P\text{-}H}$ = 21 and 12 Hz, int = 1.2), and −16.48 (Ir−$H_t$, d of d, $J_{cis\text{-}P\text{-}H}$ = 24 and 11 Hz, int = 0.9) can be assigned to a complex with two inequivalent terminal hydrides, one SH, and one $SCH_3$. Of the three possible isomers, it is presumed that the one represented by these $^1H$ NMR resonances is the ae isomer, on the basis of the comparison of relative concentrations of the isomers in analogous complexes.[30] There were also very small signals in the hydride, $SCH_3$, and SH regions that could be associated with the aa and ee isomers, or possibly a small concentration of $[Ir_2(SCH_3)_2(H)_3(PPh_3)_4]^+$, but this could not be definitively determined.

## Experimental Section

**Physical Measurements and Reagents.** Infrared spectra were recorded on either a Mattson Cygnus FTIR or a Beckman Model 4250 grating spectrophotometer equipped with a HgCdTe detector with use of KBr pellets. UV–vis spectra were recorded on a Cary 17D spectrophotometer. $^1H$ and $^{31}P$ NMR spectra were recorded at 300 and 121.5 MHz, respectively, with a Nicolet NT-300 spectrometer. Chemical shifts are reported as $\delta$ values with positive shifts downfield. $^{31}P$ NMR spectra were run with proton decoupling and are reported as $\delta$ values relative to the external standard 85% $H_3PO_4$. Elemental analyses were performed by Galbraith Laboratories, Inc., Knoxville, TN. Iridium trichloride hydrate was obtained from Johnson-Matthey, Inc. $[Ir(H)_2(Me_2CO)_2(PPh_3)_2]BF_4$ was synthesized according to published procedures.[38] All solvents were reagent grade and were used without further purification. $H_2S$ was purchased from Matheson Gas Co. and used as purchased. $Bu_4NPF_6$ was purchased from Southwestern Analytical Chemicals, Inc., and used without further purification. All manipulations were carried out under a purified nitrogen atmosphere by using standard Schlenk line techniques.

**Synthesis of the Compounds.** $[Ir_2(SH)_2(H)_3(PPh_3)_4]BF_4$ **(1)** was prepared by stirring a colorless solution of $[Ir(H)_2(Me_2CO)_2(PPh_3)_2]BF_4$ (245 mg, 0.266 mmol) in 10 mL of acetone under an $H_2S$ atmosphere for 10 min. The color changed immediately to yellow with the evolution of gas bubbles. The volume was reduced slightly by blowing a stream of $N_2$ over the solution. A yellow powder was isolated upon the addition of $Et_2O$ (a yellow oil upon the addition of hexane). After the solvent was decanted, the product was washed with ca. $^1/_2$ mL of acetone, producing an orange solution. This was repeated with small portions of acetone several times until the solution was no longer orange, but yellow. These

(37) Shaver, A.; Fitzpatrick, P. J.; Steliou, K.; Butler, I. S. *J. Am. Chem. Soc.* **1979**, *101*, 1313.

(38) Crabtree, R. H.; Hlatky, G. G.; Parnell, C. P.; Segmüller, B. E.; Uriarte, R. J. *Inorg. Chem.* **1984**, *23*, 354.

**Table I.** Summary of Crystal Data and Intensity Collection for $[Ir_2(SH)_2(H)_3(PPh_3)_4]BF_4 \cdot 2(CH_3)_2CO$ (**1**·2$(CH_3)_2CO$), $[Ir_2S(SH)(H)_3(PPh_3)_4] \cdot 1.5C_6H_6$ (**2**·1.5$C_6H_6$), and $[Ir_2(SH)(SC_3H_7)(H)_3(PPh_3)_4]BF_4 \cdot (CH_3)_2CO$ (**3**·$(CH_3)_2CO$)

| | **1** | **2** | **3** |
|---|---|---|---|
| | | Crystal Parameters | |
| cryst syst | triclinic | monoclinic | monoclinic |
| space group | $P\bar{1}$ | $P2_1/n$ | $P2_1/a$ |
| cryst dimens, mm | 0.15 × 0.2 × 0.25 | 0.2 × 0.2 × 0.25 | 0.3 × 0.25 × 0.3 |
| cell params (25 °C) | | | |
| $a$, Å | 14.919 (8) | 17.377 (6) | 20.154 (9) |
| $b$, Å | 23.63 (2) | 24.658 (6) | 18.349 (9) |
| $c$, Å | 18.835 (4) | 18.220 (5) | 21.690 (7) |
| $\alpha$, deg | 92.09 (5) | 90 | 90 |
| $\beta$, deg | 113.95 (4) | 92.76 (2) | 108.08 (3) |
| $\gamma$, deg | 79.16 (7) | 90 | 90 |
| $V$, Å$^3$ | 4056 (8) | 7798 (7) | 7625 (8) |
| $Z$ | 2 | 4 | 4 |
| calcd density, g/cm$^3$ | 1.396 | 1.379 | 1.472 |
| abs coeff, cm$^{-1}$ | 34.4 | 35.7 | 36.6 |
| max, min av transmission factors | 1.0, 0.81, 0.93 | 1.0, 0.84, 0.93 | 1.0, 0.82, 0.91 |
| formula | $Ir_2S_2P_4F_4O_2C_{78}BH_{77}$ | $Ir_2S_2P_4C_{81}H_{73}$ | $Ir_2S_2P_4F_4OC_{78}BH_{77}$ |
| fw | 1705.71 | 1618.91 | 1689.71 |
| | | Measurement of Intensity Data (25 °C) | |
| diffractometer | | CAD 4 | |
| radiation | | Mo K$\alpha$ ($\lambda$ = 0.71069 Å), graphite monochromatized | |
| scan type; range, 2$\theta$, deg | $\omega$–2$\theta$; 0–45 | $\omega$; 8–46 | $\omega$; 0–44 |
| unique rflns measd (region) | 10607 ($+h,\pm k,\pm l$) | 10814 ($+h,+k,\pm l$) | 9702 ($+h,+k,\pm l$) |
| obsd rflns[a] | 5975 [$(F_o)^2 \geq 3\sigma(F_o)^2$] | 5030 [$(F_o)^2 \geq 3\sigma(F_o)^2$] | 6186 [$(F_o)^2 \geq 3\sigma(F_o)^2$] |
| | | Refinement by Full-Matrix Least Squares | |
| no. of params | 411 | 410 | 461 |
| $R$[b] | 0.056 | 0.046 | 0.046 |
| $R_w$[b] | 0.076 | 0.058 | 0.063 |
| GOF[b] | 2.04 | 1.41 | 2.00 |
| $P$[a] | 0.04 | 0.04 | 0.04 |

[a] The intensity data were processed as described in: *CAD4 and SDP User's Manual*; Enraf-Nonius: Delft, Holland, 1978. The net intensity $I$ is given by $I = [K/\text{NPI}](C - 2B)$, where $K$ = 20.1166(attenuator factor), NPI = ratio of fastest possible scal rate for the measurement, $C$ = total count, and $B$ = total background count. The standard deviation in the net intensity is given by $[\sigma(I)]^2 = (K/\text{NPI})^2[C + 4B + (PI)^2]$ where $P$ is a factor used to downweight intense reflections. The observed structure factor amplitude $F_o$ is given by $F_o = (I/Lp)^{1/2}$ where $Lp$ = Lorentz and polarization factors. The $\sigma(I)$'s were converted to the estimated errors in the relative structure factors $\sigma(F_o)$ by $\sigma(F_o) = {}^1/_2[\sigma(I)/I]F_o$. [b] The function minimized was $\sum w(|F_o| - |F_c|)^2$, where $w = 1/[\sigma(F_o)]^2$. The unweighted and weighted residuals are defined as $R = \sum(||F_o| - |F_c||)/\sum|F_o|$ and $R_w = [(\sum w(|F_o| - |F_c|)^2)/(\sum w|F_o|^2)]^{1/2}$. The error in an observation of unit weight (GOF) is $[\sum w(|F_o| - |F_c|)^2/(\text{NO} - \text{NV})]^{1/2}$, where NO and NV are the numbers of observations and variables, respectively.

portions of orange acetone solution were combined and layered with hexane, from which was isolated product **3** (vide infra). The remainder of the yellow product was dissolved in acetone and similarly layered with hexane. Slow crystallization produced large yellow crystalline needles in 47% yield that readily lost solvent upon removal from the mother liquor, giving an opaque yellow powder. $^{31}P$ NMR (acetone, 25 °C): $\delta$ 14.49, 14.29, 11.16, 3.46, 3.13, –0.21, –1.30 (d, $J$ = 44 Hz). $^1H$ NMR (acetone-$d_6$, 25 °C): $\delta$ 7.2 ($C_6H_5$, m, int = 122.3), 0.50 (SH, s, int = 1.0), –0.24 (SH, s, int = 0.22), –2.51 (SH, s, int = 0.98), –3.36 (SH, s, int = 1.43), –14.56 (Ir–$H_b$, m, int = 1.97), –15.65 (Ir–$H_t$, d of d, $J_{cis\text{-}P\text{-}H}$ = 21 and 12 Hz, int = 1.25), –15.86 (Ir–$H_t$, d of d, int = 0.45), –16.13 (Ir–$H_t$, d of d, $J_{cis\text{-}P\text{-}H}$ = 19 and 14 Hz, int = 2.74). Integration of $^1H$ NMR: 62:1.8:2.3:1 phenyl H:SH:Ir–$H_t$:Ir–$H_b$. IR: $\nu$(SH) = 2677, 2523 cm$^{-1}$; $\nu$(IrH) = 2195 cm$^{-1}$; $\nu(BF_4^-)$ = 1050 cm$^{-1}$. UV–vis (0.15 mM $CH_2Cl_2$): $\lambda_{max}$ = 322 nm (sh), $\epsilon$ = 9300 M$^{-1}$ cm$^{-1}$; $\lambda_{max}$ = 360 nm (sh), $\epsilon$ = 5900 M$^{-1}$ cm$^{-1}$. Anal. Calcd for $Ir_2S_2P_4F_4C_{72}BH_{65}$: C, 54.41; H, 4.12; P, 7.79; F, 4.78. Found: C, 54.77; H, 4.30; P, 7.68; F, 4.70. The P:F ratio (calculated 1.63, found 1.63) supports the formulation as a monocation.

**$[Ir_2S(SH)(H)_3(PPh_3)_4]$ (2)** was prepared by the addition of NaOMe, Na/Hg, piperidine, $Et_3N$, or sodium naphthalenide to an acetone solution of **1**. For example, 19 mg of NaOMe (0.352 mmol) and 150 mg of **1** (0.094 mmol) were stirred in a degassed acetone solution for several hours. The color changed from yellow to green with the precipitation of a green solid. This mixture was filtered and washed with several portions of MeOH to remove the excess NaOMe. The solid was dissolved in benzene and filtered. Recrystallization from benzene/hexane produced 135 mg (95% yield) of green rectangular crystals of **2** as a benzene solvate. $^{31}P$ NMR (toluene, 25 °C): $\delta$ 14.66, 9.84, 4.98 (d, $J$ = 64 Hz), 3.75 (m), 1.30 (m). $^1H$ NMR (toluene-$d_8$, 25 °C): $\delta$ 7.6, 7.0 ($C_6H_5$, m, int = 141), 0.39 (SH, s, int = 1.0), –0.91 (SH, s, int = 1.1), –12.78 (Ir–$H_b$, m, int = 3.7), –14.98 (Ir–$H_t$, d of d, $J_{cis\text{-}P\text{-}H}$ = 22 and 12 Hz, int = 2.3), –16.77 (Ir–$H_t$, d of d, $J_{cis\text{-}P\text{-}H}$ = 26 and 12 Hz, int = 1.2). Integration of $^1H$ NMR: 59:0.9:3 phenyl H:SH:Ir–H. IR: $\nu$(SH) = 2672 cm$^{-1}$ (vw); $\nu$(IrH) = 2091, 2179 cm$^{-1}$ (w). UV–vis (0.025 mM $CH_2Cl_2$): $\lambda_{max}$ = 317 nm (sh), $\epsilon$ = 13100 M$^{-1}$ cm$^{-1}$. Anal. Calcd for $Ir_2S_2P_4C_{81}H_{73}$: C, 60.09; H, 4.54; P, 7.65. Found: C, 60.32; H, 4.84; P, 7.34. The 1.5 $C_6H_6$ solvate gave the best agreement to the analytical data.

**$[Ir_2(SH)(SC_3H_7)(H)_3(PPh_3)_4]BF_4$ (3)** was also isolated from the reaction of $H_2S$ with $[Ir(H)_2(Me_2CO)_2(PPh_3)_2]BF_4$ in acetone (see preparation of compound **1**). Recrystallization from the orange acetone/hexane solution (vide supra) yielded yellow needles of **1** and large yellowish orange rectangular crystals. A Pasteur separation was carried out, giving a yield of 9.8% of the yellowish orange crystals, which lost acetone solvent very slowly upon removal from the mother liquor, resulting in cracked crystals. $^{31}P$ NMR ($CH_3CN$, 25 °C): $\delta$ 9.19, 7.34, 2.90, 0.38 (d, $J$ = 55 Hz), –0.32, –1.99, –8.50 (d, $J$ = 48 Hz). $^1H$ NMR ($CD_3CN$, 23 °C): $\delta$ 7.1 ($C_6H_5$, m), –2.4 (SH, s), –0.1 (SH, br s), 0.4 (SH and isopropyl $CH_3$, br s), 0.3 (isopropyl $CH_3$, d, $J \approx$ 6 Hz), 0.7 and 0.5 (isopropyl $CH_3$, d, $J \approx$ 6 Hz), 1.2 and 1.1 (isopropyl $CH_3$, d, $J \approx$ 6 Hz), –15.1 (Ir–$H_t$, d of d, $J_{cis\text{-}P\text{-}H}$ = 19 and 12 Hz), –16.0 (Ir–$H_b$, t of t, $J_{trans\text{-}P\text{-}H}$ = 59 Hz, $J_{cis\text{-}P\text{-}H}$ = 9 Hz), –16.6 (Ir–$H_t$, m), –16.9 (Ir–$H_t$, pseudotriplet, $J_{cis\text{-}P\text{-}H}$ = 18 Hz). Integration of $^1H$ NMR: 1:2:1:7 SH:Ir–$H_t$:Ir–$H_b$:isopropyl $CH_3$. IR: $\nu$(SH) = 2673 cm$^{-1}$; $\nu$(IrH) = 2199 cm$^{-1}$; $\nu(BF_4^-)$ = 1050 cm$^{-1}$. UV–vis (0.032 mM $CH_2Cl_2$): $\lambda_{max}$ = 320 nm (sh), $\epsilon$ = 8400 M$^{-1}$ cm$^{-1}$. Anal. Calcd for $Ir_2S_2P_4F_4C_{75}BH_{71}$: C, 55.21; H, 4.39. Found: C, 55.49; H, 4.49.

**$[Ir_2S(SC_3H_7)(H)_3(PPh_3)_4]$ (4).** An acetone solution of **3** was added to an acetone solution of NaOMe, qualitatively. The color changed within a few minutes of stirring from yellow-orange to green with the precipitation of a green solid. Recrystallization from benzene/hexane yielded green crystals. $^{31}P$ NMR (benzene, 25 °C): $\delta$ 8.9, 0.5, –0.6, –1.1, –4.9. $^1H$ NMR (benzene-$d_6$, 25 °C, major isomer): $\delta$ 2.01 (isopropyl CH, br s), 0.76 (isopropyl $CH_3$, d, $J$ = 10 Hz), –12.40 (Ir–$H_t$, t, $J$ = 15 Hz), –13.58 (Ir–$H_b$, t, $J$ = 66 Hz), –17.04 (Ir–$H_t$, d of d, $J$ = 23 and 18 Hz).

**$[Ir_2(S_2CH_2)(H)_3(PPh_3)_4]X$ (X = I, $BF_4$) (5). Method a.** $CH_2I_2$ (3.0 $\mu$L, 0.037 mmol) and $Et_3N$ (3.6 $\mu$L, 0.026 mmol) was added to an acetone solution of **1** (20 mg, 0.013 mmol) and stirred under $N_2$ for

**Table II.** Positional Parameters and Estimated Standard Deviations for Core Atoms in $[Ir_2(SH)_2(H)_3(PPh_3)_4]BF_4 \cdot 2(CH_3)_2CO$ ($\mathbf{1} \cdot 2(CH_3)_2CO$)[a]

| atom | x | y | z | B, Å² |
|---|---|---|---|---|
| Ir1 | 0.14793 (5) | 0.28442 (3) | 0.04346 (6) | 2.69 (2) |
| Ir2 | 0.28794 (5) | 0.18193 (3) | 0.08141 (6) | 2.68 (2) |
| S1 | 0.2639 (4) | 0.2436 (2) | 0.2301 (4) | 3.5 (1) |
| S2 | 0.1100 (3) | 0.1864 (2) | 0.0203 (4) | 3.3 (1) |
| P1 | 0.0628 (4) | 0.3068 (2) | −0.1486 (4) | 3.1 (1) |
| P2 | 0.0495 (4) | 0.3387 (2) | 0.1232 (4) | 3.2 (1) |
| P3 | 0.4434 (4) | 0.2017 (2) | 0.1270 (4) | 3.5 (1) |
| P4 | 0.3177 (4) | 0.0871 (2) | 0.1365 (4) | 3.0 (1) |
| C1A | −0.073 (1) | 0.3251 (8) | −0.207 (1) | 3.6 (4)* |
| C1B | 0.084 (1) | 0.2449 (8) | −0.233 (1) | 3.5 (4)* |
| C1C | 0.097 (1) | 0.3628 (8) | −0.210 (1) | 3.3 (4)* |
| C1D | −0.065 (1) | 0.3887 (9) | 0.037 (1) | 3.8 (4)* |
| C1E | 0.011 (1) | 0.2924 (8) | 0.199 (1) | 3.6 (4)* |
| C1F | 0.114 (1) | 0.3865 (8) | 0.232 (1) | 3.7 (4)* |
| C1G | 0.446 (1) | 0.2773 (9) | 0.163 (2) | 4.7 (5)* |
| C1H | 0.547 (1) | 0.1637 (9) | 0.256 (2) | 4.4 (5)* |
| C1I | 0.490 (1) | 0.1927 (9) | 0.015 (1) | 3.9 (4)* |
| C1J | 0.255 (1) | 0.0809 (8) | 0.234 (1) | 3.0 (4)* |
| C1K | 0.264 (1) | 0.0391 (8) | 0.021 (1) | 2.9 (4)* |
| C1L | 0.447 (1) | 0.0438 (8) | 0.207 (1) | 3.5 (4)* |

[a] Starred values are for atoms refined isotropically. Counterion, solvate, and remaining phenyl group positional parameters are provided in the supplementary material. Anisotropically refined atoms are given in the form of the isotropic equivalent thermal parameter defined as $^4/_3[a^2\beta(1,1) + b^2\beta(2,2) + c^2\beta(3,3) + ab(\cos\gamma)\beta(1,2) + ac(\cos\beta)\beta(1,3) + bc(\cos\alpha)\beta(2,3)]$.

several hours. After only a few minutes the solution had changed from yellow to orangish yellow. A yellow precipitate was obtained by layering the solution with hexane. Yield 73%.

**Method b.** $CH_2I_2$ (7.6 μL, 0.095 mmol) was added to a THF solution of the green dimer **2** (15 mg, 0.010 mmol) and stirred for several hours. The solution turned yellow with the formation of a pale yellow precipitate, which was filtered, washed with hexane, and dried in vacuo; yield 92%. $^{31}P$ NMR (acetone, 25 °C): δ 6.43 (s, int = 1), 5.04 (s, int = 1). $^1H$ NMR (acetone-$d_6$, 25 °C): δ 7.56 ($C_6H_5$, m), 6.09 ($S_2CH_2$, s, int = 1.8), −11.60 (Ir–$H_b$, t of t, $J_{trans\text{-}P\text{-}H}$ = 59 Hz, $J_{cis\text{-}P\text{-}H}$ = 10 Hz, int = 1), −17.79 (Ir–$H_t$, d of d, $J_{cis\text{-}P\text{-}H}$ = 23 and 14 Hz, int = 2). IR: ν(IrH) = 2180 $cm^{-1}$.

**$[Ir_2(SCH_2CH_2S)(H)_3(PPh_3)_4]X$ (X = Br, $BF_4$) (6).** $Br(CH_2)_2Br$ (12 μL, 0.15 mmol) was added to a toluene solution of **2** (30 mg, 0.02 mmol) and stirred for several hours. The solution changed from green to a pale yellow slurry. The pale yellow precipitate was collected by filtration, washed with hexane, and dried in vacuo; yield 95%. $^{31}P$ NMR (acetone, 25 °C): δ 7.43 (s, int = 1), 7.31 (s, int = 1). $^1H$ NMR (acetone-$d_6$, 25 °C): δ 7.38 ($C_6H_5$, m), 6.90 ($SCH_2CH_2S$, s, int = 6), −14.74 (Ir–$H_b$, t of t, $J_{trans\text{-}P\text{-}H}$ = 47 Hz, $J_{cis\text{-}P\text{-}H}$ = 10 Hz, int = 1), −15.01 (Ir–$H_t$, d of d, $J_{cis\text{-}P\text{-}H}$ = 25 and 13 Hz, int = 1.7). IR: ν(IrH) = 2160 $cm^{-1}$.

**$[Ir_2(SCH_3)_2(H)_3(PPh_3)_4]X$ (X = I, $BF_4$) (7). Method a.** A solution of **2** in freshly distilled THF was cooled to −78 °C. *n*-BuLi (2.1 equiv/mol of dimer) was added, followed by $CH_3I$ (5.2 equiv). As the solution was allowed to warm to room temperature, the solution changed from green to yellow. The solvent was removed in vacuo and the yellow precipitate was washed with hexane and dried in vacuo; yield 94%.

**Method b.** To an acetone solution of **1** was added a large excess of $CH_3I$ (26 equiv/mol of dimer) and 2.1 equiv of $Et_3N$. The solution was stirred overnight, during which time the color changed to a deeper yellow. The solvent was removed in vacuo, yielding a yellow precipitate, which was washed with hexane and $Et_2O$ and dried in vacuo; yield 90%. $^{31}P$ NMR (acetone, 25 °C): δ 11.23 (s, int = 1.0), 5.98 (m, int = 0.9), 1.11 (m, int = 1.1), −3.53 (s, int = 1.0). $^1H$ NMR (acetone-$d_6$, 25 °C): δ 1.09 ($SCH_3$, d, $J$ = 5 Hz, int = 3.3), 0.74 ($SCH_3$, d, $J$ = 5 Hz, int = 3.2), −14.43 (Ir–$H_b$, t of t, $J_{trans\text{-}P\text{-}H}$ = 60 Hz, $J_{cis\text{-}P\text{-}H}$ = 10 Hz, int = 1.0), −15.57 (Ir–$H_t$, d of d, $J_{cis\text{-}P\text{-}H}$ = 22 and 13 Hz, int = 1.2), −16.08 (Ir–$H_t$, d of d, $J_{cis\text{-}P\text{-}H}$ = 23 and 15 Hz, int = 1.2). IR: ν(IrH) = 2160 $cm^{-1}$.

**$[Ir_2(SH)(SCH_3)(H)_3(PPh_3)_4]X$ (X = I, $BF_4$) (8).** To a benzene solution of **2** was added either $CH_3I$ or methyl triflate (2.1 equiv/mol of dimer). The solution turned yellow immediately. The solvent was removed in vacuo, and the yellow solid was washed with hexane and $Et_2O$; yield 88%. $^{31}P$ NMR (acetone, 25 °C, major isomer): δ 13.5, 12.2, 4.8, 4.5 (all singlets of ca. equal intensity). $^1H$ NMR (acetone-$d_6$, 25 °C, major isomer): δ 0.58 ($SCH_3$, d, $J$ = 6 Hz, int = 2.7), −0.07 (SH, br s, int = 0.8), −14.37 (Ir–$H_b$, t of t, $J_{trans\text{-}P\text{-}H}$ = 59 Hz, $J_{cis\text{-}P\text{-}H}$ = 9 Hz, int = 1.0), −15.22 (Ir–$H_t$, d of d, $J_{cis\text{-}P\text{-}H}$ = 21 and 12 Hz, int = 1.2), −16.48 (Ir–$H_t$, d of d, $J_{cis\text{-}P\text{-}H}$ = 24 and 11 Hz, int = 0.9).

**Table III.** Positional Parameters and Estimated Standard Deviations for Core Atoms in $[Ir_2S(SH)(H)_3(PPh_3)_4] \cdot 1.5C_6H_6$ ($\mathbf{2} \cdot 1.5C_6H_6$)[a]

| atom | x | y | z | B, Å² |
|---|---|---|---|---|
| Ir1 | 0.32333 (3) | 0.20814 (3) | −0.02732 (3) | 2.97 (1) |
| Ir2 | 0.19632 (3) | 0.20715 (3) | 0.05953 (3) | 3.04 (1) |
| S1 | 0.2075 (2) | 0.1579 (2) | −0.0562 (2) | 3.57 (9) |
| S2 | 0.3123 (2) | 0.1571 (2) | 0.0870 (2) | 3.9 (1) |
| P1 | 0.4168 (2) | 0.2620 (2) | 0.0248 (2) | 3.5 (1) |
| P2 | 0.3859 (2) | 0.1557 (2) | −0.1070 (2) | 3.27 (9) |
| P3 | 0.1039 (2) | 0.2631 (2) | 0.0099 (2) | 3.5 (1) |
| P4 | 0.1357 (2) | 0.1527 (2) | 0.1380 (2) | 3.6 (1) |
| C1A | 0.5121 (9) | 0.2304 (7) | 0.0455 (8) | 3.9 (3)* |
| C1B | 0.3918 (8) | 0.2888 (7) | 0.1163 (8) | 3.9 (3)* |
| C1C | 0.4410 (9) | 0.3264 (6) | −0.0200 (8) | 3.9 (3)* |
| C1D | 0.4879 (8) | 0.1624 (6) | −0.1183 (8) | 3.0 (3)* |
| C1E | 0.3715 (9) | 0.0838 (7) | −0.0868 (8) | 4.1 (4)* |
| C1F | 0.3503 (8) | 0.1615 (6) | −0.2038 (8) | 3.2 (3) |
| C1G | 0.1284 (8) | 0.2887 (7) | −0.0808 (8) | 3.7 (3)* |
| C1H | 0.0078 (9) | 0.2326 (6) | −0.0089 (8) | 3.7 (3)* |
| C1I | 0.0825 (9) | 0.3265 (7) | 0.0566 (9) | 4.7 (4)* |
| C1J | 0.1498 (9) | 0.0807 (7) | 0.1195 (9) | 4.5 (4)* |
| C1K | 0.1712 (9) | 0.1563 (7) | 0.2346 (8) | 4.1 (4)* |
| C1L | 0.0316 (9) | 0.1584 (7) | 0.1507 (9) | 4.5 (4)* |

[a] See footnote *a* of Table II.

**Table IV.** Positional Parameters and Estimated Standard Deviations for Core Atoms in $[Ir_2(SH)(SC_3H_7)(H)_3(PPh_3)_4]BF \cdot (CH_3)_2CO$ ($\mathbf{3} \cdot (CH_3)_2CO$)[a]

| atom | x | y | z | B, Å² |
|---|---|---|---|---|
| Ir1 | 0.19539 (3) | 0.04360 (3) | 0.31037 (2) | 3.01 (1) |
| Ir2 | 0.25335 (3) | −0.01677 (3) | 0.21893 (2) | 3.12 (1) |
| S1 | 0.2021 (2) | 0.1050 (2) | 0.2146 (2) | 4.05 (9) |
| S2 | 0.1405 (2) | −0.0474 (2) | 0.2257 (2) | 3.94 (8) |
| P1 | 0.2183 (2) | −0.0144 (2) | 0.4081 (2) | 3.29 (8) |
| P2 | 0.1109 (2) | 0.1239 (2) | 0.3173 (2) | 3.72 (9) |
| P3 | 0.3665 (2) | 0.0243 (2) | 0.2410 (2) | 3.39 (8) |
| P4 | 0.2340 (2) | −0.0565 (2) | 0.1136 (2) | 4.4 (1) |
| C1 | 0.1313 (7) | −0.1402 (8) | 0.2573 (7) | 5.1 (4) |
| C2 | 0.0521 (8) | −0.158 (1) | 0.2288 (9) | 7.4 (5) |
| C3 | 0.174 (1) | −0.1978 (9) | 0.2375 (8) | 7.8 (5) |
| C1A | 0.2274 (6) | 0.0438 (7) | 0.4792 (6) | 3.5 (3)* |
| C1B | 0.3015 (7) | −0.0618 (7) | 0.4317 (6) | 3.9 (3)* |
| C1C | 0.1583 (7) | −0.0827 (7) | 0.4185 (6) | 3.8 (3)* |
| C1D | 0.0532 (7) | 0.1038 (8) | 0.3667 (7) | 4.7 (3)* |
| C1E | 0.1439 (7) | 0.2168 (8) | 0.3444 (7) | 4.3 (3)* |
| C1F | 0.0469 (8) | 0.1413 (8) | 0.2369 (7) | 5.0 (3)* |
| C1G | 0.3949 (7) | 0.0540 (7) | 0.1721 (6) | 4.0 (3)* |
| C1H | 0.4378 (7) | −0.0366 (7) | 0.2869 (6) | 3.8 (3)* |
| C1I | 0.3846 (7) | 0.1053 (7) | 0.2940 (6) | 3.6 (3)* |
| C1J | 0.3055 (8) | −0.1101 (9) | 0.1060 (7) | 5.3 (4)* |
| C1K | 0.2115 (7) | 0.0076 (8) | 0.0462 (7) | 4.4 (3)* |
| C1L | 0.1535 (8) | −0.1151 (9) | 0.0818 (8) | 6.0 (4)* |

[a] See footnote *a* of Table II.

**Electrochemistry.** Electrochemical measurements of $[Ir_2(SH)_2(H)_3(PPh_3)_4]BF_4$ (**1**) were performed with a Bioanalytical Systems (BAS) Model 100 electrochemical analyzer. A three-electrode configuration consisting of a highly polished glassy-carbon-disk working electrode (area 0.07 $cm^2$), a platinum-spiral auxiliary electrode, and a Ag/AgCl reference electrode containing 1.0 M KCl was used. The working compartment of the electrochemical cell was separated from the auxiliary compartment by a fritted-glass salt bridge and from the reference compartment by a modified Luggin capillary. All three compartments contained a 0.1 M solution of the supporting electrolyte tetra-*n*-butylammonium hexafluorophosphate (TBAH) in spectral grade acetone.

Electrolyte solutions were prepared and stored over 80–200 mesh activated alumina prior to use in experiments. Working solutions were prepared by recording background cyclic voltammograms of 30.0 mL of the electrolyte solution before adding the sample of interest. The working compartment of the cell was bubbled with solvent-saturated argon to deaerate the solution. Potentials were measured relative to an uncorrected Ag/AgCl reference electrode. No *iR* compensation was used.[39]

(39) Gagne, R. R.; Koval, C. A.; Kisensky, G. C. *Inorg. Chem.* **1980**, *19*, 2854.

**Table V.** Selected Distances and Angles in $[Ir_2(SH)_2(H)_3(PPh_3)_4]BF_4 \cdot 2(CH_3)_2CO$ (**1**·$2(CH_3)_2CO$), $[Ir_2S(SH)(H)_3(PPh_3)_4] \cdot 1.5C_6H_6$ (**2**·$1.5C_6H_6$), and $[Ir_2(SH)(SC_3H_7)(H)_3(PPh_3)_4]BF_4 \cdot (CH_3)_2CO$ (**3**·$(CH_3)_2CO$)[a]

| | 1 | 2 | 3 |
|---|---|---|---|
| | Distances (Å) | | |
| Ir1–Ir2 | 2.796 (1) | 2.777 (1) | 2.822 (1) |
| Ir1–S1 | 2.416 (3) | 2.401 (3) | 2.404 (3) |
| Ir1–S2 | 2.462 (4) | 2.449 (4) | 2.475 (3) |
| Ir1–P1 | 2.296 (4) | 2.270 (4) | 2.288 (3) |
| Ir1–P2 | 2.294 (4) | 2.261 (4) | 2.292 (3) |
| Ir2–S1 | 2.459 (4) | 2.449 (4) | 2.450 (3) |
| Ir2–S2 | 2.415 (4) | 2.396 (4) | 2.391 (3) |
| Ir2–P3 | 2.286 (4) | 2.273 (4) | 2.308 (3) |
| Ir2–P4 | 2.281 (4) | 2.259 (4) | 2.313 (3) |
| S1–S2 | 3.193 (5) | 3.110 (5) | 3.098 (4) |
| S2–C1 | | | 1.87 (1) |
| C1–C2 | | | 1.56 (2) |
| C1–C3 | | | 1.50 (2) |
| P1–C1A | 1.82 (2) | 1.85 (2) | 1.84 (1) |
| P1–C1B | 1.85 (2) | 1.86 (2) | 1.81 (1) |
| P1–C1C | 1.81 (2) | 1.84 (2) | 1.80 (1) |
| P2–C1D | 1.82 (2) | 1.80 (2) | 1.85 (1) |
| P2–C1E | 1.80 (2) | 1.83 (2) | 1.86 (1) |
| P2–C1F | 1.83 (2) | 1.85 (2) | 1.85 (1) |
| P3–C1G | 1.83 (2) | 1.84 (2) | 1.84 (1) |
| P3–C1H | 1.86 (2) | 1.85 (2) | 1.85 (1) |
| P3–C1I | 1.82 (2) | 1.83 (2) | 1.85 (1) |
| P4–C1J | 1.87 (2) | 1.82 (2) | 1.80 (1) |
| P4–C1K | 1.84 (2) | 1.84 (2) | 1.82 (1) |
| P4–C1L | 1.87 (2) | 1.84 (2) | 1.89 (1) |
| | Angles (deg) | | |
| S1–Ir1–S2 | 81.8 (1) | 79.8 (2) | 78.8 (1) |
| S1–Ir1–P1 | 165.8 (1) | 165.7 (1) | 165.8 (1) |
| S1–Ir1–P2 | 90.1 (1) | 89.4 (1) | 89.9 (1) |
| S2–Ir1–P1 | 92.0 (1) | 91.6 (1) | 106.8 (1) |
| S2–Ir1–P2 | 108.6 (1) | 108.2 (1) | 108.2 (1) |
| P1–Ir1–P2 | 104.1 (1) | 104.3 (1) | 100.3 (1) |
| S1–Ir2–S2 | 81.9 (1) | 79.9 (1) | 79.6 (1) |
| S1–Ir2–P3 | 92.1 (2) | 92.4 (1) | 95.1 (1) |
| S1–Ir2–P4 | 110.0 (1) | 108.0 (1) | 108.0 (1) |
| S2–Ir2–P3 | 165.7 (1) | 165.4 (1) | 164.2 (1) |
| S2–Ir2–P4 | 90.1 (1) | 88.6 (1) | 96.6 (1) |
| P3–Ir2–P4 | 104.2 (2) | 105.7 (1) | 99.2 (1) |
| Ir1–S1–Ir2 | 70.0 (1) | 69.9 (1) | 71.08 (7) |
| Ir1–S2–Ir2 | 70.0 (1) | 69.9 (1) | 70.88 (7) |
| Ir1–P1–C1A | 118.3 (5) | 117.0 (5) | 116.5 (3) |
| Ir1–P1–C1B | 111.1 (5) | 113.0 (5) | 112.8 (3) |
| Ir1–P1–C1C | 118.2 (5) | 119.5 (5) | 119.3 (3) |
| Ir1–P2–C1D | 121.6 (5) | 121.9 (5) | 121.6 (4) |
| Ir1–P2–C1E | 110.1 (5) | 110.5 (5) | 114.2 (4) |
| Ir1–P2–C1F | 114.2 (5) | 114.8 (5) | 111.4 (4) |
| Ir2–P3–C1G | 110.6 (5) | 112.1 (4) | 117.7 (3) |
| Ir2–P3–C1H | 117.3 (5) | 116.2 (5) | 117.8 (3) |
| Ir2–P3–C1I | 116.5 (5) | 119.3 (5) | 112.5 (3) |
| Ir2–P4–C1J | 108.2 (5) | 113.0 (5) | 111.7 (4) |
| Ir2–P4–C1K | 115.1 (5) | 115.6 (5) | 120.9 (4) |
| Ir2–P4–C1L | 122.2 (5) | 121.7 (5) | 113.7 (4) |
| Ir1–S2–C1 | | | 114.6 (4) |
| Ir2–S2–C1 | | | 116.2 (4) |
| S2–C1–C2 | | | 104.5 (9) |
| S2–C1–C3 | | | 114.0 (8) |
| C2–C1–C3 | | | 110 (1) |

[a] The numbering schemes are identical for all three compounds.

**Collection and Reduction of X-ray Data.** A summary of crystal and intensity collection data for the solvates of **1–3**, $[Ir_2(SH)_2(H)_3(PPh_3)_4]BF_4 \cdot 2(CH_3)_2CO$, $[Ir_2S(SH)(H)_3(PPh_3)_4] \cdot 1.5C_6H_6$, and $[Ir_2(SH)(SC_3H_7)(H)_3(PPh_3)_4]BF_4 \cdot (CH_3)_2CO$, is presented in Table I. A yellow crystal of **1** and a yellow-orange crystal of **3** were secured inside 0.2-mm sealed capillary tubes, each of which contained a small amount of acetone. A green crystal of **2** was secured on a thin glass fiber with use of epoxy resin. The crystal of **1** was found to belong to the triclinic space group $P\bar{1}$ and those of **2** and **3** were found to belong to the monoclinic space groups $P2_1/n$ and $P2_1/a$, respectively, by the Enraf-Nonius CAD4-SDP peak search, centering, and indexing programs, by systematic absences observed during data collection, and by successful solution and refinement (vide infra).[40] The space groups were unambiguously determined for all three compounds. The unit cell dimensions were determined by least-squares refinement of the angular settings of 25 peaks centered on the diffractometer. The intensities of three standard reflections were measured every 1.5 h of X-ray exposure, and no decay with time was noted. The data were corrected for Lorentz, polarization, and background effects. The data of absorption were included with use of the empirical absorption program EAC ($\psi$-scan data).[40]

**Solution and Refinement of the Structures.** The structures were solved by conventional heavy-atom techniques. The metal atoms were located by Patterson synthesis. Full-matrix least-squares refinement and difference Fourier calculations were used to locate all remaining non-hydrogen atoms. Phenyl ring hydrogen atoms were calculated in idealized positions and were included during the final stages of refinement for the structures of **1** and **2**. Hydrogen atoms were not included in any refinement of **3**. The final difference Fourier maps did not reveal any chemically significant residual electron density. Peaks were not observed in the regions expected for the iridium hydrides or for the sulfhydryl hydrogens, and therefore these atoms were not included. Difference Fourier maps based on low-angle data were also calculated but did not provide evidence for location of the hydride positions. The crystals of both **1** and **3** contained two acetone solvate molecules per cation and one $BF_4^-$ anion, the latter of which showed the usual signs of disorder. Refinement with anisotropic thermal parameters for the fluorine atoms gave reasonable values for distances and angles. The two acetone solvate molecules located for **3** converged to give occupancy factors of 0.5 for each upon refinement, resulting in an overall 1.0 acetone solvate formulation. The crystal of **2** contained two benzene solvate molecules for each diiridium molecule. Refinement of these benzene solvate molecules converged to a 0.75 occupancy for each, thus giving an overall 1.5 benzene solvate formulation. This was in agreement with elemental analysis.

The atomic scattering factors were taken from the usual tabulation,[41] and the effects of anomalous dispersion were included in $F_c$ by using Cromer and Ibers' values of $\Delta f'$ and $\Delta f''$.[42] Corrections for extinction were not applied. The final positional and thermal parameters of the refined atoms of the cations, including only the first carbon of the phenyl rings, appear in Tables II–IV. Selected distances and angles for complexes **1–3** are listed in Table V. ORTEP drawings of the cations including the labeling schemes are shown in Figures 1 and 2. A complete listing of thermal parameters, refined positional parameters, calculated positions for the hydrogen atoms, distances, angles, least-squares planes, and structure factor amplitudes are included as supplementary material.

**Acknowledgment.** This work was supported by the National Science Foundation. We also thank the Johnson Matthey Co. for generous loans of iridium salts. A.M.M. thanks Allied Chemical and Louise T. Dosdall Foundation for fellowships.

**Supplementary Material Available:** Tables S1–S12, listing all bond distances and angles, general temperature factor expressions, final atom positional and thermal parameters, and least-squares planes, and Figures S1–S5, showing the ORTEP representations of the cations with labeling schemes as well as detailed analyses of the $^1H$ NMR spectra of **2** and **3** and the $^{31}P$ NMR spectrum of **3** (44 pages); Tables S13–S15, listing observed and calculated structure factors (70 pages). Ordering information is given on any current masthead page.

(40) All calculations were carried out on PDP 8A and 11/34 computers with use of the Enraf-Nonius CAD 4-SDP-PLUS programs. This crystallographic computing package is described by: Frenz, B. A. In *Computing in Crystallography*; Schenk, H., Olthoff-Hazekamp, R., van Konigsveld, H., Bassi, G. C., Eds.; Delft University Press: Delft, Holland, 1978; pp 64–71. *Structure Determination Package and SDP-PLUS User's Guide*; B. A. Frenz & Associates: College Station, TX, 1982.
(41) Cromer, D. T.; Waber, J. T. *International Tables for X-Ray Crystallography*; Kynoch: Birmingham, England, 1974; Vol. IV, Table 2.2.4.
(42) Cromer, D. T. *International Tables for X-Ray Crystallography*; Kynoch: Birmingham, England, 1974; Vol. IV, Table 2.3.